Journal of Solid State Chemistry **166,** 271–276 (2002)
doi:10.1006/jssc.2002.9574

# Valence States and Luminescence Properties of Ytterbium Ions in Strontium Haloborates

V. P. Dotsenko,*[,1] I. V. Berezovskaya,* P. V. Pyrogenko,* N. P. Efryushina,* P. A. Rodnyi,†
C. W. E. van Eijk,‡ and A. V. Sidorenko‡

**Physico-Chemical Institute, Ukrainian Academy of Sciences, 86 Lustdorfskaya doroga, 65080 Odessa, Ukraine; †State Technical University, Polytechnicheskaya 29, 195251 St. Petersburg, Russia; and ‡Interfaculty Reactor Institute, Delft University of Technology, Mekelweg 15, 2629 JB Delft, The Netherlands*

Received November 20, 2001; in revised form February 14, 2002; accepted March 1, 2002

**The luminescence properties of ytterbium ions in strontium haloborates were studied under optical, X-ray and synchrotron excitation. The coexistence of Yb ions in two valence states (divalent and trivalent) was detected in the $Sr_2B_5O_9X$:Yb ($X$ = Cl, Br) powder materials prepared in a slightly reducing ($H_2/N_2$) or an oxidizing atmosphere. Under optical excitation, the $5d \rightarrow 4f$ $Yb^{2+}$ luminescence at 420 nm is observed. Even under X-ray excitation, an emission band with a maximum of about 340 nm appears in the spectra. This broadband emission is attributed to charge transfer luminescence of $Yb^{3+}$. The influence of the structural features of $Sr_2B_5O_9X$ and some preparative conditions of the samples on the luminescent behavior of Yb are discussed.** © 2002 Elsevier Science (USA)

*Key Words:* **strontium haloborates; ytterbium; luminescence.**

## 1. INTRODUCTION

In recent years, materials of composition $M_2B_5O_9X$:$Eu^{2+}$ ($M$ = Ca, Sr, Ba; $X$ = Cl, Br) gained special attention because of possible applications as storage phosphors for X-ray imaging (1) and thermal-neutron detection (2, 3). The results obtained on their photostimulated luminescence are consistent with a model in which halide vacancies act as electron traps and $Eu^{2+}$ is involved in the hole trapping. However, the results are quite complicated and a full understanding of the physical processes responsible for the storage properties of these materials requires significant additional studies.

It is known that the $Yb^{2+}$ ion in $SrB_4O_7$ shows a very efficient luminescence due to $4f^{13}5d \rightarrow 4f^{14}$ transitions (4). The emission band has a maximum at 362 nm, at 300 K. This fact prompted us to test the ability of ytterbium-containing $M_2B_5O_9X$ to be used as storage phosphors for thermal-neutron detection. In this paper, we report on the luminescence of $Yb^{2+}$ and $Yb^{3+}$ ions in strontium haloborates. It is widely accepted that the crystal structure of $Sr_2B_5O_9X$ ($X$ = Cl, Br) does not differ significantly from that of $Eu_2B_5O_9Br$ for which Machida *et al.* (5) have given a detailed description. The crystal structure of $Eu_2B_5O_9Br$ consists of a three-dimensional $(B_5O_9)_\infty$ network in which $B_5O_{12}$ groups of three $BO_4$ tetrahedra and two $BO_3$ triangles are linked together (5). The europium ions are surrounded by seven oxygen ions and two halogen ions. The average Eu–O and Eu–Br distances are 2.7 and 3.0 Å, respectively.

## 2. EXPERIMENTAL

The $Sr_{2(1-x)}Yb_{2x}B_5O_9X$ ($x$ = 0.001, 0.01) solid solutions were prepared using a standard solid-state method. Starting mixtures of $SrCO_3$, $SrX_2 \cdot nH_2O$ (10% excess), $Yb(NO_3)_3$ and $H_3BO_3$ (15% excess) were fired at a temperature of about 400°C for 1 h and then at 750–800°C for 3 h in a nitrogen stream. The samples were cooled, mortared to insure homogeneity and fired again at 800°C for 2 h in a reducing atmosphere consisting of a nitrogen–hydrogen mixture containing 5% by volume of hydrogen. The samples were analyzed in the as-prepared state and after annealing at 700°C for 2 h in air. The annealing was applied to stimulate conversion of $Yb^{2+}$ into $Yb^{3+}$ and, therefore, for the study of the $Yb^{3+}$ response. All the samples were checked by X-ray diffraction (XRD) using Cu$K\alpha$ radiation. No impurity phases were detected in the XRD patterns. The emission and excitation spectra were recorded at 300 K using an LOMO SDL 1 spectrofluorometer equipped with a xenon lamp. The spectra were corrected for the photomultiplier sensitivity and the monochromator efficiency using a calibrated light source. For the decay time measurements, a flash xenon lamp and a pulsed YAG:$Nd^{3+}$ laser ($\lambda_{exc}$ = 266 nm) were employed. The measurements of

---

[1] To whom correspondence should be addressed. Fax: 38 (0482) 652012. E-mail: physchem@paco.net.

excitation spectra at wavelengths shorter than 240 nm were performed at room temperature using synchrotron radiation and the equipment of the SUPERLUMI experimental station (6) of HASYLAB (Hamburg, Germany). These spectra were corrected for the wavelength-dependent excitation intensity with the use of sodium salicylate as a standard. X-ray-induced emission spectra were recorded using an X-ray tube with a Cu anode operated at 35 kV and 25 mA. For thermally stimulated luminescence (TSL) measurements, an $Sr^{90}/Y^{90}$ $\beta$-source installed in a Risø TL/OSL-DA 15 A/B reader was applied. The dose rate was 1.0 mGy/s in air. Since the luminescent properties of samples with $x = 0.001$ and 0.01 were found to be the same, we will report only those for $x = 0.01$ samples.

## 3. RESULTS

Figure 1 shows the emission and UV excitation spectra of $Sr_{2(1-x)}Yb_{2x}B_5O_9Cl$ ($x = 0.01$) sample in the as-prepared state. The emission spectrum consists of a single band with a maximum at about 420 nm. In the excitation spectrum of this emission several bands at 267, 305, 338 and 374 nm are observed. These bands must be ascribed to transitions between the $4f^{14}$ and $4f^{13}5d$ configurations of the $Yb^{2+}$ ion. No significant change of the 420 nm emission is observed upon varying the excitation wavelength in the 240–380 nm region. It is hard to determine the Stokes shift of this emission, because the corresponding excitation band can be too weak to be observed (4, 7) and no fine structure is observed in the excitation spectrum at 300 K. A rough estimate of the Stokes shift can be obtained by assuming that the excitation band is the mirror image of the emission band. In this way, we obtain a value of about 3000 cm$^{-1}$, which is typical for $4f^n \rightarrow 4f^{n-1}5d$ transitions. Upon direct excitation of the $Yb^{2+}$ ions in the 260–375 nm range, the decay of the emission is single-exponential with a time constant of $30 \pm 2$ μs. It is important to note that the emission and excitation spectra of $Sr_{2(1-x)}Yb_{2x}B_5O_9Br$ appear to be identical to those observed for the $Sr_{2(1-x)}Yb_{2x}B_5O_9Cl$ samples. Also, it was found that the annealing of the samples in air suppresses the 420 nm emission, but not completely.

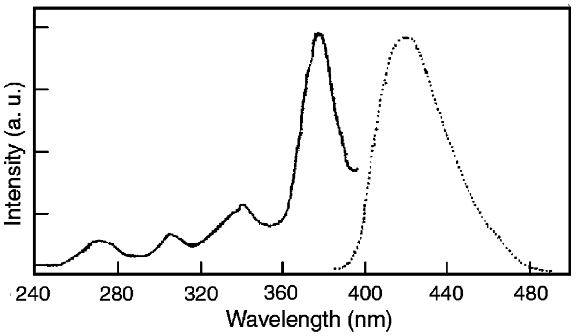

**FIG. 1.** Emission and excitation spectra of $Sr_{2(1-x)}Yb_{2x}B_5O_9Cl$ ($x = 0.01$) at 300 K. The emission spectrum (---) was recorded upon excitation at 340 nm. The excitation spectrum (——) was recorded for emission at 420 nm.

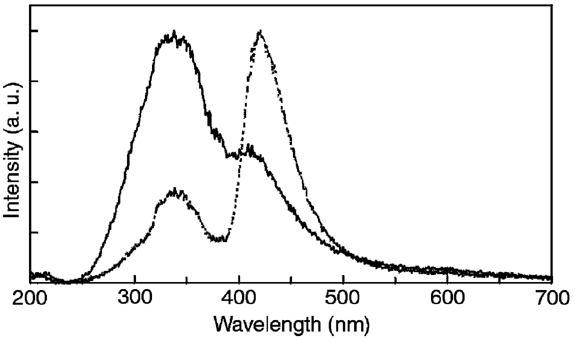

**FIG. 2.** Comparison of X-ray-induced emission spectra of $Sr_{2(1-x)}Yb_{2x}B_5O_9Br$ ($x = 0.01$) at 300 K. (---) as-prepared sample; (——) oxidized sample.

The X-ray-induced emission spectra of $Sr_{2(1-x)}Yb_{2x}B_5O_9Br$ ($x = 0.01$) at room temperature are shown in Fig. 2. It is evident that these spectra are quite different from that shown in Fig. 1. The emission extends from 250 to 600 nm and has two maxima at 340 and 420 nm. As can be seen from Fig. 2, the annealing of the sample in air significantly reduces the long-wavelength peak. The spectra show, in addition, sharp peaks at 980 nm, which could not be observed upon UV excitation. It is evident that these features are due to the transitions between the two $4f$ states of $Yb^{3+}$. The X-ray-induced emission spectra of the $Sr_{2(1-x)}Yb_{2x}B_5O_9Cl$ samples show the same characteristics.

Figure 3 shows the (V)UV excitation spectrum of the 420 nm emission of $Sr_{2(1-x)}Yb_{2x}B_5O_9Cl$ ($x = 0.01$) in the as-prepared state. It is evident that the excitation bands in the 4-6 eV region are due to the direct excitation of the $Yb^{2+}$ ions via transitions to the components of the $Yb^{2+}$ $5d$ configuration. Also, there is a weak band with a maximum at about 6.53 eV (190 nm). Excitation into this band yields the spectrum in which the 347 nm band dominates (see inset in Fig. 3). The origin of this excitation band will be discussed below. The local maximum at about 7.52 eV (165 nm) can be assigned to a band gap transition with a subsequent energy transfer to the $Yb^{2+}$ ions. Between 8 and 16 eV, the emission intensity continues to increase with increasing excitation energy. Note that in the 7–18 eV region the excitation spectrum is similar to that for $Sr_2B_5O_9X$ doped with either $Ce^{3+}$ (8) or $Eu^{2+}$ (9).

Figure 4 shows the time-resolved excitation spectra of the UV emission at 350 nm of $Sr_{2(1-x)}Yb_{2x}B_5O_9Cl$ ($x = 0.01$) after annealing at 700°C for 2 h in air. The short-time excitation spectrum consists of a band starting at about 5.90 eV (210 nm) and peaking at 6.70 eV (185 nm). Note that

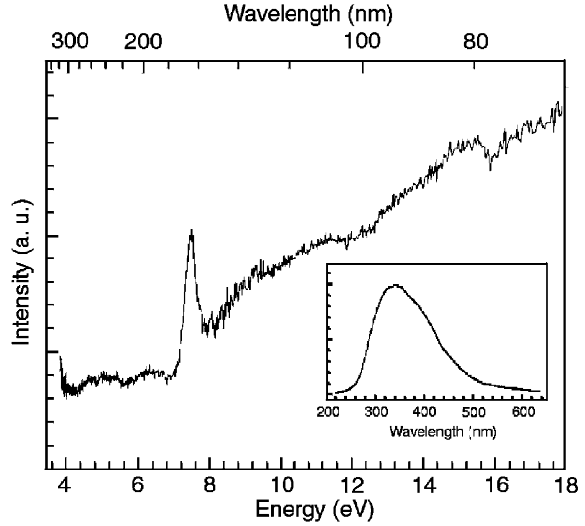

**FIG. 3.** (V)UV excitation spectrum of $Sr_{2(1-x)}Yb_{2x}B_5O_9Cl$ ($x = 0.01$) monitoring the blue emission ($\lambda_{em} = 420$ nm) at 300 K. The inset shows the emission spectrum upon excitation at 180 nm.

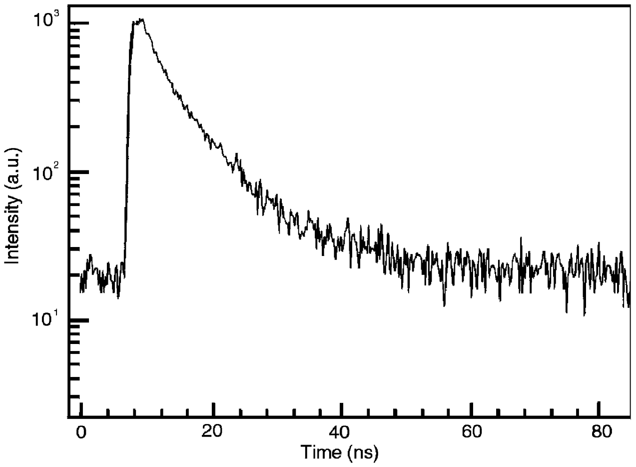

**FIG. 5.** Decay curve of the emission at 350 nm of $Sr_{2(1-x)}Yb_{2x}B_5O_9Br$ ($x = 0.01$) in the as-prepared state recorded upon excitation at 180 nm, $T = 300$ K.

this band is not observed in the excitation spectra of strontium haloborates doped with $Ce^{3+}$ or $Eu^{2+}$. The weak luminescence intensity for excitation energies larger than 7.6 eV indicates that energy transfer from the generated electron–hole pairs to centers responsible for the UV emission is not efficient. The time-delayed excitation spectrum has a more complicated structure. In addition to the 6.7 eV excitation band, there is a sharp increase of the emission intensity between 7.2 and 7.8 eV. The local maximum at about 7.8 eV can be assigned to a band gap transition with a subsequent energy transfer to the impurity ions.

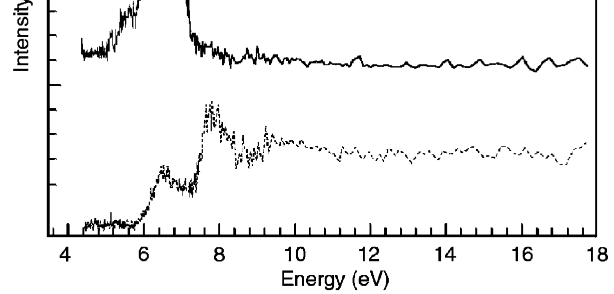

**FIG. 4.** Time-resolved excitation spectra of $Sr_{2(1-x)}Yb_{2x}B_5O_9Cl$ ($x = 0.01$) monitoring the UV emission ($\lambda_{em} = 350$ nm) at 300 K. The spectra were recorded for two different time intervals after picosecond pulse excitation; (——) between 1 and 10 ns, and (- - -) between 50 and 200 ns.

The decay curve of the UV emission of $Sr_{2(1-x)}Yb_{2x}B_5O_9Cl$ ($x = 0.01$) for the 180 nm excitation wavelength is presented in Fig. 5. Upon excitation at $\lambda_{exc} = 180$ nm (6.88 eV), the decay shows a strong deviation from exponential behavior. It is evident that its duration is much shorter than the decay time of the 420 nm emission. The time required for the luminescence to decay to 1/e of its initial intensity was found to be 5 ns.

After exposure of the samples to $\beta$-radiation, a TSL signal is observed. The TSL spectra of $Sr_{2(1-x)}Yb_{2x}B_5O_9Br$ ($x = 0.01$) appear to be similar to the X-ray-induced emission spectra (Fig. 2), indicating that the TSL originates from Yb-related centers. Figure 6 shows the TSL glow curves of the $Sr_{2(1-x)}Yb_{2x}B_5O_9Br$ ($x = 0.01$) samples after $\beta$-irradiation for 60 s at room temperature. A stronger peak at about 350 K and a weaker one with a maximum at about 405 K are observed. Note that the peak positions are in good agreement with those obtained for $Sr_2B_5O_9Br{:}Eu^{2+}$ (2). The resemblance between the TSL glow curves can be seen as the evidence that the same types of trapping and recombination mechanisms are involved.

## 4. DISCUSSION

Depending upon the method of preparation, Yb can enter as $Yb^{2+}$ or $Yb^{3+}$ in strontium haloborates. It is evident that the blue emission band which shows the decrease in intensity upon annealing in air originates from $Yb^{2+}$-related exciting and emitting centers. The luminescent properties of $Yb^{2+}$ in alkaline earth sulfates and alkaline earth halides

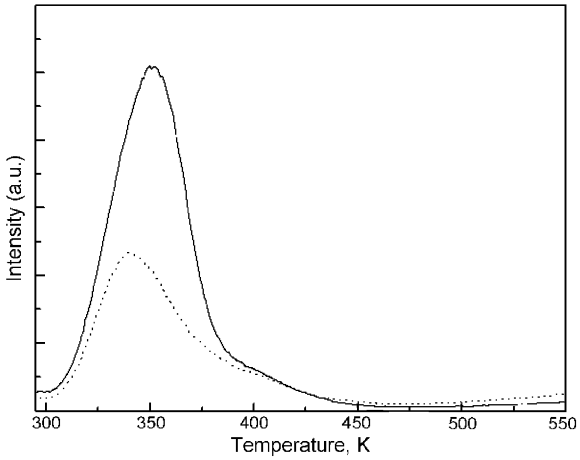

**FIG. 6.** TSL glow curves of $\beta$-irradiated $Sr_{2(1-x)}Yb_{2x}B_5O_9Br$ ($x = 0.01$) for the integrated emission; (——) as-prepared sample; and (- - -) oxidized sample. The heating rate is 1 K/s.

have been reported in the literature (7,10,11). The emission spectra are ascribed to $5d \rightarrow 4f$ transitions on the $Yb^{2+}$ ions or to $Yb^{2+}$ trapped exciton emission. The $Yb^{2+}$ $5d \rightarrow 4f$ emission is usually between 360 and 450 nm. The blue emission with the maximum at 420 nm is between these extremes and shows the characteristics of $Yb^{2+}$ emission. The red shift with respect to the lowest excitation band is small ($3000\,cm^{-1}$), the decay time ($\tau$) at 300 K is relatively long (30 μs). Note that this value of $\tau$ is larger than that found for $Ce^{3+}$ (30–40 ns) (8), $Sm^{2+}$ and $Eu^{2+}$ (1–6 μs) (9) in these lattices. This observation agrees with the proposition made by Lizzo *et al.* (7) that the contraction of the $4f$ orbitals on the heavier lanthanide ions reduces the overlap between the delocalized $5d$ orbital and the $4f$ orbital, resulting in lower transition probabilities. The strong resemblance between the emission and UV excitation spectra for $Sr_2B_5O_9X{:}Yb^{2+}$ ($X$ = Cl, Br) indicates that the energy position of the $Yb^{2+}$-levels in strontium haloborates is mainly determined by the influence of neighboring oxygen ions belonging to the borate groups, and not by the two halogen ions. For $Ce^{3+}$ and $Eu^{2+}$ ions in these host lattices, the stronger nephelauxetic effect of $Br^-$ in comparison with $Cl^-$ causes the shift to longer wavelengths of the excitation and emission bands of the impurity ions in the bromoborates compared to the chloroborates (8).

Several explanations can be put forward to interpret the emission with $\lambda_{max} = 340$ nm (Fig. 2). It is obvious to assume that this emission is related to $Yb^{3+}$ ions. Reports on the energy position of the $5d$ states of $Yb^{3+}$ ions are restricted to a few of fluoride compounds. For $CaF_2$ and $BaY_2F_8$, an absorption band at about 141 nm has been reported (12,13). Recently, it has been shown that the depression of the $5d$ level ($\Delta\, Ln^{3+}$) in a crystal is approximately constant along the lanthanide series (14, 15). Dorenbos (14) finds this depression to be the same for all the $Ln^{3+}$ ions, within $600\,cm^{-1}$. This allows one to estimate the energy position of the $5d$ states of any lanthanide ion. By choosing $E$ ($Ce^{3+}$, free) $= 49{,}737\,cm^{-1}$ and $E$ ($Yb^{3+}$, free) $= 80{,}200\,cm^{-1}$ (16) and taking into account that for $Sr_2B_5O_9Cl$ $\Delta\, Ce^{3+} = 17{,}500\,cm^{-1}$ (8), we can obtain a value of 7.6 eV (165 nm) as the energy position of the lowest $4f \rightarrow 5d$ transition on $Yb^{3+}$ ion in $Sr_2B_5O_9X$. Since the fundamental absorption edge of $Sr_2B_5O_9X$ ($X$ = Cl, Br) is at 7.2 eV, the $5d$ excited states of $Yb^{3+}$ are expected to lie in the conduction band. It is clear that these states cannot be responsible for the 6.70 eV (185 nm) excitation band.

Another explanation is that the 340 nm emission is caused by transition from the charge transfer state (CTS) of $Yb^{3+}$ ions to the $^2F_{7/2}$ state of $Yb^{3+}$. Since the separation between the $^2F_{7/2}$ and $^2F_{5/2}$ states of $Yb^{3+}$ is about $10{,}000\,cm^{-1}$, the CTS $\rightarrow$ $^2F_{5/2}$ emission band is expected to be at 540 nm. This band seems to be hidden on the longer wavelength side of the 340 nm emission. In this connection, we point out that the CTS $\rightarrow$ $^2F_{7/2}$ emission band is often significantly more intense than the band corresponding to the CTS $\rightarrow$ $^2F_{5/2}$ transition. Let us now compare the charge transfer (CT) band energies of $Yb^{3+}$-doped strontium chloroborate and other host lattices. Recently, van Pieterson *et al.* (17) have reported the first systematic study of $Yb^{3+}$ CT luminescence in a large variety of rare-earth ($RE^{3+}$) compounds. In $LiYF_4$ a CT absorption band was found to be at a high energy (7.8 eV), while in oxidic systems at lower energies ($\approx$5.5 eV). It was shown that the CTS $\rightarrow$ $^2F_{7/2}$ emission bands are broad and the Stokes shift of the emission varies from $7000\,cm^{-1}$ for $RE_2O_2S$ and $LiYF_4$ to $17{,}000\,cm^{-1}$ for $Y_2O_3$ and $Y_3Al_5O_{12}$. It is evident that the CT excitation band of $Yb^{3+}$ in $Sr_2B_5O_9Cl$ is at a relatively high energy, viz. 6.70 eV (185 nm), and the Stokes shift of the CT emission is large ($25{,}000\,cm^{-1}$). It is known that the coordination and the size of cation site influence the energy of the CT transition (16,17). It is generally accepted that the average metal–ligand distance represents the size of the site. One may expect that an increase in metal–ligand distance will cause an increase in the energy required for a CT transition. Taking into account that the average metal–ligand distance ($R$) in $Sr_2B_5O_9X$ is 2.70 Å (4), we can conclude that the cation sites are essentially larger in $Sr_2B_5O_9X$ than in $Y_2O_3$ ($R_{Y\text{-}O} = 2.28$ Å) and $Y_3Al_5O_{12}$ ($R_{Y\text{-}O} = 2.37$ Å). The excitation spectra of $Eu^{3+}$ emission in $Sr_2B_5O_9X$ show a broad band in the UV spectral region (2,18). This band was attributed to a charge transfer transition of $Eu^{3+}$-ligand complexes. Knitel *et al.* (2) reported the value of 5.77 eV (215 nm) as a maximum of the CT band of $Sr_2B_5O_9Br{:}Eu^{3+}$. The shift of the CT band to lower energies for $Eu^{3+}$ in comparison to $Yb^{3+}$ is in agreement with the results of van Pieterson *et al.* (17) for other systems. The size of the site available to the $Yb^{3+}$ also affects the relaxation in the CTS. When $Yb^{3+}$ is incorporated in a lattice on a larger cationic site, the relaxation in the charge transfer state is larger and therefore the Stokes shift is larger. The observation of the $\mathrm{Yb}^{3+}$ CT luminescence in $\mathrm{Sr_2B_5O_9}X$ was unexpected because in $RE\mathrm{BO_3}$ ($RE$ = Sc, Y, La) no $\mathrm{Yb}^{3+}$ charge transfer luminescence was observed even at 10 K (17). The higher quenching temperature for the CT luminescence from $\mathrm{Yb}^{3+}$ can be related to the higher stability of $\mathrm{Yb}^{2+}$ in $\mathrm{Sr_2B_5O_9}X$ compared to $RE\mathrm{BO_3}$. To verify this hypothesis new experiments on ytterbium-doped alkaline earth borates ($M\mathrm{B_4O_7}$, $M\mathrm{B_2O_4}$, etc.) are planned. It should be noted that the CT luminescence of $\mathrm{Yb}^{3+}$ offers favorable possibilities to apply $\mathrm{Yb}^{3+}$-based materials for solar neutrino detection (19).

The asymmetrical shape of the excitation band at 185 nm (Fig. 4) indicates that the observed spectrum consists of at least two superimposed spectra due to different $\mathrm{Yb}^{3+}$ complexes present in the sample. When $\mathrm{Yb}^{3+}$ ions are doped into strontium haloborates they substitute for strontium ions and therefore require charge compensation to maintain the overall charge neutrality of the crystal. In our previous work on $\mathrm{Ce}^{3+}$ in these host lattices (8) it was found that the dominant charge compensation mechanism in $\mathrm{Sr_2B_5O_9}X{:}\mathrm{Ce}^{3+}$ ($X$ = Cl, Br) solid solutions includes the formation of one vacancy per two rare-earth ions incorporated. This process can be described by the Kröger–Vink notation:

$$3\mathrm{Sr}_{\mathrm{Sr}}^{\times} \rightarrow 2\mathrm{Ce}_{\mathrm{Sr}}^{\bullet} + V_{\mathrm{Sr}}''. \qquad [1]$$

Here, the subscript "Sr" denotes an ion in a strontium site in the lattice. The superscripts •, × and ″ denote, respectively, +1, 0 and −2 formal charges of defects relative to the lattice. Therefore, the asymmetric shape of the 185 nm excitation band can be explained by the existence of several kinds of ytterbium centers in $\mathrm{Sr_2B_5O_9}X$, namely the isolated $\mathrm{Yb}^{3+}$ center and the associated pair center of $\mathrm{Yb}^{3+}$ and strontium vacancy. Such a situation was reported for $\mathrm{Eu}^{3+}$ ions in CaO (20, 21). The CT bands of $\mathrm{CaO{:}Eu}^{3+}$ have been observed at 235 nm for the $\mathrm{Eu}_{\mathrm{Ca}}^{\bullet}$ center and at 250 nm for the associated pair center of $\mathrm{Eu}^{3+}$ and cation vacancy. Also, it is likely that the annealing of the samples in air leads to the appearance of centers in which the charge compensation is realized by the substitution of an $\mathrm{O}^{2-}$ on one of the halogen sites, i.e. $(\mathrm{Yb_{Sr}}\cdot\mathrm{O_X})^{\times}$ associates. Since the excitation bands of the $\mathrm{Yb}^{3+}$ centers in $\mathrm{Sr_2B_5O_9}X$ show a considerable overlap, we were not able to accomplish a fully selective excitation and record the emission of any center exclusively.

The CT nature of the radiative center responsible for the 340 nm emission is supported by the fast decay of a few nanoseconds. The radiative lifetime of the $\mathrm{Yb}^{3+}$ CT emission is typically between 100 and 200 ns (17). At room temperature, the decay time is 10–20 ns due to the increase with temperature of nonradiative transitions to the $\mathrm{Yb}^{3+}$ ground state. From Figs. 1 and 2 it follows that there is a considerable spectral overlap between the CT emission band from $\mathrm{Yb}^{3+}$ and the excitation bands of $\mathrm{Yb}^{2+}$ ions in $\mathrm{Sr_2B_5O_9}X$. This overlap suggests that energy transfer between the corresponding centers can take place. As a result, the nonexponential decay of the CT emission of $\mathrm{Yb}^{3+}$ is observed (Fig. 5). Thus, by accepting the CT nature of the 340 nm emission, we can explain our experimental data.

TSL measurements were made for $\mathrm{Sr}_{2(1-x)}\mathrm{Yb}_{2x}\mathrm{B_5O_9Br}$ ($x = 0.01$) in the as-prepared state, i.e., before oxidation of $\mathrm{Yb}^{2+}$ ions and in the oxidized state, after substantial conversion to $\mathrm{Yb}^{3+}$. The TSL spectra appear to be similar to the X-ray-induced emission spectra, indicating that the TSL originates from the $\mathrm{Yb}^{2+}$ and $\mathrm{Yb}^{3+}$ centers. A comparison of the TSL glow curves (Fig. 6) seems to show that the main trapping states are due to intrinsic lattice defects of these materials. A more detailed study of the trapping processes in this host lattice is beyond the scope of this work.

## 5. CONCLUSION

The luminescence properties of ytterbium ions in strontium haloborates were studied under optical, X-ray and synchrotron excitation. The coexistence of Yb ions in two valence states (divalent and trivalent) was detected in the $\mathrm{Sr_2B_5O_9}X{:}\mathrm{Yb}$ ($X$ = Cl, Br) powder materials prepared in a slightly reducing ($\mathrm{H_2/N_2}$) or an oxidizing atmosphere. The $\mathrm{Yb}^{2+}$ ions give rise to the emission band at 420 nm. The $\mathrm{Yb}^{3+}$ ions cause the emission band at about 340 nm. This emission band is attributed to charge transfer luminescence of $\mathrm{Yb}^{3+}$. The study of the storage properties of $\mathrm{Sr}_{2(1-x)}\mathrm{Yb}_{2x}\mathrm{B_5O_9}X$ solid solutions is in progress at Delft University of Technology.

## ACKNOWLEDGMENTS

The authors are grateful to Dr. Voloshinovskii for performing the experiments at the synchrotron of Hamburg.

## REFERENCES

1. A. Meijerink and G. Blasse, *J. Phys. D: Appl. Phys.* **24,** 626 (1991).
2. M. Knitel, "New inorganic scintillators and storage phosphors for detection of thermal neutrons," Ph.D Thesis, Delft University of Technology, 1998.
3. M. J. Knitel, B. Hommels, P. Dorenbos, C. W. E. van Eijk, I. Berezovskaya, and V. Dotsenko, *Nucl. Instrum. Methods A* **449,** 595 (2000).
4. G. Blasse, G. J. Dirksen, and A. Meijerink, *Chem. Phys. Lett.* **167,** 41 (1990).
5. K. Machida, G. Adachi, N. Yasuoka, N. Kasai, and J. Shiokawa, *Inorg. Chem.* **19,** 3807 (1980).
6. G. Zimmerer, *Nucl. Instrum. Methods A* **308,** 178 (1991).
7. S. Lizzo, A. Meijerink, and G. Blasse, *J. Lumin.* **59,** 185 (1994).
8. V. P. Dotsenko, I. V. Berezovskaya, N. P. Efryushina, A. S. Voloshovslii, P. Dorenbos, and C. W. E. van Eijk, *J. Lumin.* **93,** 137 (2001).

9. V. P. Dotsenko, V. N. Radionov, and A. S. Voloshinovskii, *Mat. Chem. Phys.* **57,** 134 (1998).
10. E. G. Reut, *Opt. Spectrosc.* **40,** 55 (1976).
11. D. S. McClure and C. Pedrini, *Phys. Rev. B* **32,** 8465 (1985).
12. T. Szczurek and M. Schlesinger, *in* "Rare Earths Spectroscopy" (B. Jezowska-Trzebiatowska, J. Legedziewicz, and W. Strek, Eds), p. 309. World Scientific, Singapore, 1985.
13. L. I. Devyatkova, O. N. Ivanova, V. V. Mikhailin, S. N. Rudnev, B. P. Sobolev, T. V. Uvarova, and S. P. Chernov, *Sov. Phys. Dokl.* **30,** 687 (1985).
14. P. Dorenbos, *J. Lumin.* **91,** 91 (2000).
15. M. Bettinelli and R. Moncorge, *J. Lumin.* **92,** 287 (2001).
16. R. Reisfeld and C. K. Jorgensen, "Lasers and Excited States of Rare Earths." Springer-Verlag, Berlin-Heidelberg-New York, 1977.
17. L. van Pieterson, M. Heeroma, E. de Heer, and A Meijerink, *J. Lumin.* **91,** 177 (2000).
18. M. J. Knitel, P. Dorenbos, J. Andriessen, C. W. E. van Eijk, I. Berezovskaya, and V. Dotsenko, *Radiat. Meas.* **29,** 327 (1998).
19. N. Guerassimova, N. Garnier, C. Dujardin, A. G. Petrosyan, and C. Pedrini, *Chem. Phys. Lett.* **339,** 197 (2001).
20. D. Van der Voort, A. Imnof, and G. Blasse, *J. Solid State Chem.* **96,** 311 (1992).
21. N. Yamashita, *J. Electrochem. Soc.* **140,** 840 (1993).